Proceedings of 25th Conference
on Decision and Control
Athens, Greece • December 1986

DESIGN EXAMPLES USING μ-SYNTHESIS: SPACE SHUTTLE LATERAL AXIS FCS DURING REENTRY

John Doyle [1] Kathryn Lenz [2] Andy Packard [3]

Honeywell Inc., Systems and Research Center, Minneapolis, Minnesota

Abstract

This paper studies the application of Structured Singular Values (SSV or μ) for analysis and synthesis of the Space Shuttle lateral axis flight control system (FCS) during reentry. While this is a fairly standard FCS problem in most respects, the aircraft model is highly uncertain due to the poorly known aerodynamic characteristics (e.g. aero coefficients). Comparisons are made of the conventional FCS with alternatives based on H_∞ optimal control and μ-synthesis. The problem as formulated is particularly interesting and challenging because the uncertainty is large and highly structured.

1. Introduction

During reentry the Shuttle FCS is in automatic mode using a series of S-turns to reduce speed below Mach 1. The flight condition we will consider is at Mach .9, just prior to the heading alignment circle (HAC), which lines the Shuttle up on the runway for landing. Potential robustness problems were found at this flight condition in a previous study ([M1],[M2]) done at Honeywell's Systems and Research Center (SRC) for the Space and Strategic Avionics Division (SSAvD), who are responsible for validation of the Shuttle FCS.

The SRC study was a preliminary investigation of the use of μ in analyzing robustness of the Shuttle FCS, where the dominant uncertainty is modeled as large parameter variations in 9 key aerodynamic coefficients. SSAvD is now using μ to augment conventional analysis, which essentially involves trial and error using coefficient combinations known to produce problems. The potential advantage in using μ is that it is faster and more reliable than trying to search the high dimensional parameter space for bad coefficient values. Furthermore, μ analysis [D1] can be combined with H_∞ optimal control methods [F1] to produce a synthesis method, called μ-synthesis [D3], which provides H_∞ performance in the presence of structured uncertainty.

This paper reports on a study at SRC using μ-synthesis to redesign the flight control laws. The objective was to mimic the performance characteristics of the existing FCS (referred to as BrandX throughout this paper), while providing this performance for a wider range of uncertainty. The resulting controller, referred to as Musyn, thus has better robust performance. The problem was simplified to some extent to focus attention on the dominant features that were found to be the most significant problems in the actual system. The performance objective of the FCS is to execute bank commands with turn coordination in the presence of gust disturbances using aileron (actually differential elevon) and rudder (the yaw jets are turned off at Mach 1). Sensor noise, large uncertainty in the the aerodynamic coefficients, penalties on actuator magnitude, rate, and acceleration, and delays to represent effects of sampling were included. The major neglected practical issues are the effects of vehicle flexibility and nonlinearities. While these are important and significantly complicate the final design, they do not change the results in any qualitative way. It is important to emphasize that this brief study is intended only to illustrate the use of μ and is not a definitive treatment of the Shuttle FCS.

The authors are also affiliated with 1) Caltech, 2) Univ. of Minnesota, and 3) U.C., Berkeley. This work has been supported by Honeywell IRAD Funding, ONR Research Grant N00014-82-C-0157, and AFOSR Research Grant F49620-86-C-0001.

The paper is organized into 6 sections. Sections 2 and 3 briefly review μ analysis and synthesis and Section 4 describes the problem formulation. The review is minimal, covering only those methods that were actually used, and in no way claims to be a review of the robust control theory field. Section 5 begins with an analysis of BrandX along with an H_∞ controller that neglects uncertainty and gives slightly better performance but essentially no robustness. The Musyn design dramatically improves robust performance with only a slight loss of nominal performance. Comparison are made using μ and time responses. Section 6 has conclusions and an appendix is included with realizations of the aircraft model and the BrandX controller. Enough data is included in this paper so that, at least in principle, all results could be reproduced.

2. Analysis Review

This section will very briefly review the basic frequency-domain methods for analyzing the performance and robustness properties of feedback systems using μ ([D1],[D3],[D4],[M1]). The general framework to be used in this paper is illustrated in the diagram in Figure 1a. Any linear interconnection of inputs, outputs, commands, perturbations, and a controller can be rearranged to match this diagram. For the purpose of analysis the controller can be viewed as just another system component and the diagram reduces to that in figure 1b. The uncertainty in ν and Δ as well as the performance specifications on e are assumed to be normalized to 1. This requires that all weighting functions and scalings have been absorbed into the interconnection structure G. We will consider performance objectives expressed in terms of $\|G_{22}\|_\infty = \sup_\omega \bar{\sigma}(G_{22}(j\omega))$. Recall that robust stability for unstructured uncertainty (only $\bar{\sigma}(\Delta) < 1$ is known) depends on $\|G_{11}\|_\infty$. Unfortunately, norm bounds are inadequate in dealing with robust performance and realistic models of plant uncertainty involving structure; more complicated mathematical objects involving μ are required.

Figure 1a General Framework

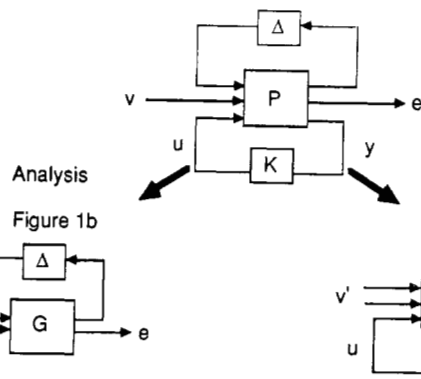

Analysis

Figure 1b

$$F_u(G,\Delta) = \left[G_{22} + G_{21}\,\Delta\,(I - G_{11}\Delta)^{-1}G_{21}\right]$$

Synthesis

Figure 1c

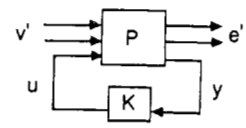

$$F_l(P,K) = \left[P_{11} + P_{12}K\,(I - P_{22}K)^{-1}P_{21}\right]$$

To begin with, assume that Δ belongs to a set like

$$\underline{\Delta} = \{ diag(\Delta_1,\Delta_2, \ldots ,\Delta_n) \} \quad \text{or} \quad \underline{B\Delta} = \{\Delta \in \underline{\Delta} \mid \bar{\sigma}(\Delta) < 1\} \quad (2.1)$$

The function μ has the properties $\mu(\alpha M) = |\alpha| \mu(M)$ and

$$det(I-M\Delta)\neq 0 \quad \forall \ \Delta \in \underline{B\Delta} \quad \text{iff} \quad \mu(M) \leq 1. \quad (2.2)$$

Obviously, μ is a function of M which depends on the *structure* of $\underline{\Delta}$. For this informal discussion just keep this fact in mind since the structure will always be clear from context. Let

$$\underline{U} = \{diag(U_1,U_2, \ldots ,U_n) \mid U_i^* U_i = I\} \quad (2.3)$$

$$\underline{D} = \{diag(d_1 I,d_2 I,\ldots,d_n I) \mid d_i \in \mathbb{R}+\} \quad (2.4)$$

where the sets $\underline{U}$ and $\underline{D}$ match the structure of $\underline{\Delta}$. Note that the $\underline{U}$ and $\underline{D}$ leave $\underline{\Delta}$ invariant in the sense that $\Delta \in \underline{\Delta}$, $U \in \underline{U}$ and $D \in \underline{D}$ implies that $\bar{\sigma}(\Delta U) = \bar{\sigma}(U\Delta) = \bar{\sigma}(\Delta)$ and $D\Delta D^{-1} = \Delta$. The sets $\underline{U}$ and $\underline{D}$ can be used to obtain the bounds

$$\max_{U \in \underline{U}} \rho(MU) \leq \mu(M) \leq \inf_{D \in \underline{D}} \bar{\sigma}(DMD^{-1}) \quad (2.5)$$

where ρ denotes the spectral radius and $\bar{\sigma}$ denotes the maximum singular value.

The key theorems about μ show that the lower bound is always an equality and the upper bound is an equality when $n \leq 3$. Unfortunately, the optimization problem implied by the lower bound has multiple local maxima so it does not immediately yield a reliable computational approach. Although $\bar{\sigma}(DMD^{-1})$ is convex in $\ln(D)$ so that the infimum can be found by search over $n-1$ real parameters, the infimum is not necessarily equal to μ (i.e., an example of strict inequality has been found for $n = 4$). On the other hand, extensive experimentation indicates that the upper bound may be close to μ in general, although this has not been proven. The worst case ratio of lower over upper bound found so far is .85. For all the cases in this paper, μ is equal to the upper bound.

Another important aspect of the upper bound is that μ may be viewed as $\bar{\sigma}$ plus scaling. Thus the general synthesis methods developed for H_∞ optimization may be applied, via scalings, to optimize μ. This will be discussed further in the synthesis square blocks, but it is easy to extend μ to handle both nonsquare and repeated blocks, although the notation becomes cumbersome.

The importance of μ for studying robustness of feedback systems is due to the following two theorems, which characterize in terms of μ the robust stability and robust performance of a system in the presence of structured uncertainty.

Theorem RS (Robust Stability)

$$\mathbf{F}_u(G,\Delta) \text{ stable } \forall \Delta \in \underline{B\Delta} \text{ iff } \sup_\omega \mu(G_{11}(j\omega)) \leq 1$$

Theorem RP (Robust Performance)

$$\mathbf{F}_u(G,\Delta) \text{ stable and } \|\mathbf{F}_u(G,\Delta)\|_\infty \leq 1 \ \forall \Delta \in \underline{B\Delta}$$

$$\text{iff } \sup_\omega \mu(G(j\omega)) \leq 1$$

(where μ in Theorem RP is computed with respect to the structure $\underline{\Delta} = \{ diag(\Delta,\Delta_{n+1}) \mid \Delta \in \underline{\Delta}\}$).

3. Synthesis Review

The basic framework for the general H_∞ optimal control problem ([D2],[D3],[C2],[F1]) is shown in figure 1c. For a review of H_∞ theory, see [F1]. The objective is to find a stabilizing K which minimizes $\|\mathbf{F}_l(P,K)\|_\infty$. The first step is to find J such that $\mathbf{F}_l(P,\mathbf{F}_l(J,Q)) = \mathbf{F}_l(T,Q) = T_{11}-NQ\tilde{N} \in RH_\infty$ is stable and affine for any $Q \in RH_\infty$. We are interested in a particular J which results in N and $\tilde{N}$ being inner and co-inner respectively. That is, $N^*N = I$ and $\tilde{N}\tilde{N}^* = I$. This requires a coprime factorization with inner numerator [C1]. In addition, we require $N_\perp$ and $\tilde{N}_\perp$ inner so that $\begin{bmatrix} N & N_\perp \end{bmatrix}$ and $\begin{bmatrix} \tilde{N} \\ \tilde{N}_\perp \end{bmatrix}$ are *square* and inner. Then

$$\left\| T_{11}-NQ\tilde{N} \right\|_\infty = \left\| \begin{bmatrix} N & N_\perp \end{bmatrix}^* [T_{11}-NQ\tilde{N}] \begin{bmatrix} \tilde{N} \\ \tilde{N}_\perp \end{bmatrix}^* \right\|_\infty = \left\| \begin{bmatrix} R_{11}-Q & R_{12} \\ R_{21} & R_{22} \end{bmatrix} \right\|_\infty . \quad (3.1)$$

The standard approach to minimizing (3.1) over Q involves the so-called γ-iteration, which is computationally intensive. The alternative used in this paper is to simply choose Q to minimize $\|R_{11}-Q\|_\infty$. This provides a good approximation and is relatively cheap computationally [C2].

The μ analysis and H_∞ synthesis methods combine to produce μ-synthesis. Recall that μ may be obtained by scaling and applying $\|\bullet\|_\infty$, so that a reasonable approach is to "solve"

$$\min_{K,D} \|DF_l(P,K)D^{-1}\|_\infty \quad (3.2)$$

by iteratively solving for K and D. With either K or D fixed, the global optimum in the other variable may be found using the μ and H_∞ solutions described previously. Unfortunately, this iterative scheme is not guaranteed to find the global optimum of (3.2). Nevertheless, the approach appears promising and substantial progress is being made in developing methods to obtain the global optimum [D4].

4. Problem Description

The performance objective of the Musyn FCS is to mimic the BrandX FCS but with better robustness. Since BrandX was not designed by H_∞ techniques, and since H_∞ performance objectives only make practical sense when they include meaningful variables and weights, it is necessary to carefully reinterpret the BrandX performance in terms of weighted H_∞ performance objectives. Fortunately, the mathematical properties of H_∞ make this process relatively easy. Besides, the performance specifications for a typical FCS translate fairly naturally into the H_∞ context. Based on consultation with engineers familiar with the Shuttle FCS each disturbance, command, noise, error, and actuator variable was given simple, reasonable weights. These weights were then adjusted until each variable made an equal contribution to the $\|\bullet\|_\infty$ norm for the BrandX closed loop system. This approach finesses the problem of selecting weighted H_∞ performance objectives exclusively from physical considerations, an issue which will not be considered in this paper. Because flexible effects have been neglected in the problem formulation, the BrandX controller was simplified by removing bending mode filters.

The 4-state rigid body aircraft model has state variables and measurements

$$x_{state} = \begin{bmatrix} \beta \\ p \\ r \\ \phi \end{bmatrix} = \begin{bmatrix} \text{sideslip angle} \\ \text{roll rate} \\ \text{yaw rate} \\ \text{bank angle} \end{bmatrix} \quad \text{and} \quad y_{meas} = \begin{bmatrix} p \\ r \\ n_y \\ \phi \end{bmatrix} \quad (4.1)$$

where n_y is lateral acceleration. See Figure 2 for definitions of the variables. Angle of attack is denoted by α and V is the velocity vector.

Figure 2.

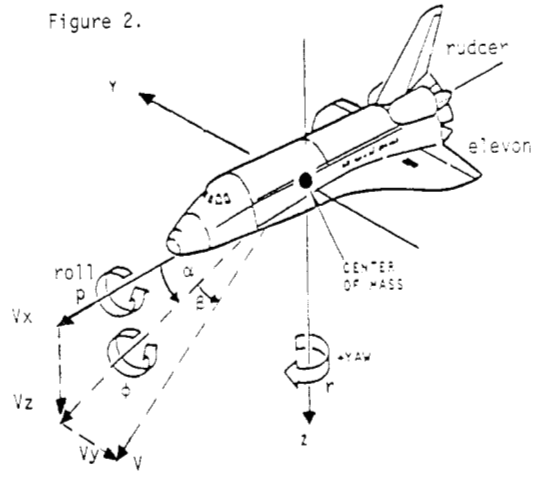

The units used throughout the paper are *rad/s* for p and r, ft/s^2 for n_y, *ft/s* for the gust, and *rad* for ϕ except in the plots where *deg* and *deg/s* replace *rad* and *rad/sec*. Each measurement is corrupted by additive sensor noise which becomes more severe with increasing frequency. Since p and r are both measured with comparable gyroscopes, their sensor noise weights are assumed to be identical and equal to $3\times10^{-3}(1+s/.01)/(1+s/.5)$. The measurement for ϕ is obtained from a navigation package at a reduced sample rate so its weight of $7\times10^{-3}(1+s/.01)/(1+s/2)$ was chosen to be relatively large in mid to high frequencies. An alternative scheme would have been to introduce a frequency-dependent perturbation to reflect the effects of sampling. The weight for the n_y accelerometer is $.25(1+s/.05)/(1+s/10)$. The sensor noise weighting filters are the increasing Bode magnitude plots shown in Figure 3.

The additional external inputs are the command in ϕ and a lateral gust disturbance weighted by $.5(1+s/2)/(1+s/.5)$ and $30*(1+s/2)/(1+s)$, respectively. Performance is described in terms of

$$e_{perf} = W_{perf}\begin{bmatrix} n_y \\ r_p \\ \phi-\phi_{ideal} \end{bmatrix} \qquad (4.2)$$

where n_y and $r_p = r - .037\phi$, the error from nominal turn rate are regulated to provide turn coordination. The ϕ_{ideal} is generated by an "ideal" model response $1/(1+2\zeta(s/\omega)+(s/\omega)^2)$ with $\omega = 1.2$ *rad/s* and $\zeta = .7$. An "ideal" turn would produce $\phi = \phi_{ideal}$ with no sensed acceleration and no turn rate error ($n_y = r_p = 0$). Of course, the vehicle physics prevents such an ideal maneuver and a good control system seeks to approach the ideal. In most conventional lateral axis control designs, n_y and r_p are blended to form a single turn coordination variable, because from a loop-shaping perspective it is easier to work with two instead of three performance variables to match the two inputs. Since we will not be using loop-shaping in this paper such "squaring down" is unnecessary. The W_{perf} performance weights are the decreasing functions plotted in Figure 3. The general shape of the weights indicates our desire to provide good performance in the low to mid frequency range. Frequencies below .01 rad are generally neglected since signals in this range are too slow to have an impact on the Shuttle reentry and landing. The performance weights are

$$W_{perf} = diag(.8\frac{(1+s)}{(1+s/.1)}, 500\frac{(1+s)}{(1+s/.01)}, 250\frac{(1+s)}{(1+s/.01)}).$$

The actuator models are second-order lags of the form $1/(1+2\zeta(s/\omega)+(s/\omega)^2)$ with $\omega = 21$ *rad/s* and $\zeta = .75$ for the rudder and $\omega = 14$ *rad/s* and $\zeta = .72$ for the elevon. To reflect practical saturation considerations actuator position, rate, and acceleration (in radians and seconds) are weighted by (2,.2,.009) respectively for rudder and (4,1,.005) for elevon. A second-order delay approximation of $(1-2\zeta(s/\omega)+(s/\omega)^2)/(1+2\zeta(s/\omega)+(s/\omega)^2)$, $\omega = 173$, $\zeta = .866$ was also included in each actuator to model the effects of the digital implementation of the controller. Although such a model is simplistic, experience has shown that it is entirely adequate for this type of study.

The major uncertainty in this problem is in the aerodynamic coefficients. These coefficients are standard aerodynamic parameters which express incremental forces and torques generated by incremental changes in sideslip, aileron, and rudder angles. Thus

$$\begin{bmatrix} \text{side force} \\ \text{yawing moment} \\ \text{rolling moment} \end{bmatrix} \propto \begin{bmatrix} c_{y\beta} & c_{ya} & c_{yr} \\ c_{n\beta} & c_{na} & c_{nr} \\ c_{l\beta} & c_{la} & c_{lr} \end{bmatrix} \begin{bmatrix} \text{sideslip angle} \\ \text{aileron angle} \\ \text{rudder angle} \end{bmatrix} \qquad (4.3)$$

The coefficients $c_{\bullet\bullet}$ are typically estimated from theoretical predictions, numerical calculations, and experiments in wind tunnels and/or flight tests. The Shuttle at Mach .9 is in a transonic regime involving a mixture of subsonic and supersonic flows. Neither the theoretical, computational, or wind tunnel techniques are particularly accurate at this flight condition, so with extremely limited flight data the coefficient uncertainty for the Shuttle is unusually large.

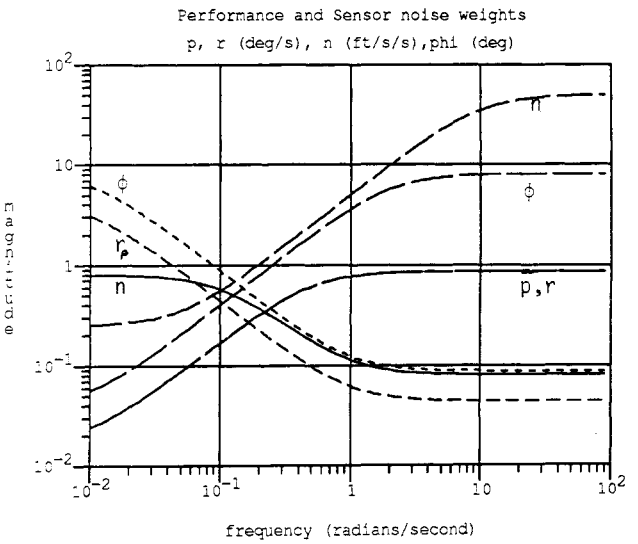

Uncertainty is modeled by representing each coefficient by a nominal value plus a perturbation. In terms of the coefficient matrix in (4.3), the perturbation may be written as

$$\begin{bmatrix} r_{y\beta}\delta_{y\beta} & r_{ya}\delta_{ya} & r_{yr}\delta_{yr} \\ r_{n\beta}\delta_{n\beta} & r_{na}\delta_{na} & r_{nr}\delta_{nr} \\ r_{l\beta}\delta_{l\beta} & r_{la}\delta_{la} & r_{lr}\delta_{lr} \end{bmatrix} = \begin{bmatrix} 3_{\bullet\beta} R_{\bullet a} R_{\bullet r} \end{bmatrix} \begin{bmatrix} diag(\delta_{\bullet\beta},\delta_{\bullet a},\delta_{\bullet r}) \end{bmatrix}$$

Each 3×1 vector $\delta_{\bullet\beta}$, $\delta_{\bullet a}$, $\delta_{\bullet r}$ is assumed to be of Euclidean norm 1, so our perturbation matrix is 9×3. The groupings on the perturbations is motivated by expected correlations between the uncertainties. Alternatively, we could, of course, ignore this and use a diagonal 9×9 perturbation. The R weightings are $R_{\bullet\beta} = diag(\ 2.194, -1.517, -.7180\ )$, $R_{\bullet a} = diag(\ -1.327,\ 1.347,\ .5185\ )$, $R_{\bullet r} = diag(\ -.3656,\ .8667,\ .2393\ )$, which are (conservative) current estimates of the size of the corresponding aero coefficient. The signs are simply arbitrary choices.

One conventional way to view the δ's is as fixed but unknown real parameters. This assumes that the rigid body dynamics are perfectly described by one 4th order model, but we simply do not know a priori which one. An alternative view is that since the coefficients represent the generation of aerodynamic forces and moments, they are actually themselves dynamical systems. Furthermore, they depend in complicated, nonlinear ways on quantities which are time-varying. We will not try to resolve this issue here but simply point out that these two views lead to apparently quite different uncertainty models. Roughly speaking, the former constrains the δ's to be real while the latter would suggest that they be complex with possibly frequency-dependent magnitude bounds. Since our μ-based methods are inherently complex, we will take the conservative approach and treat the δ's as complex. We have relatively crude extensions to μ which treat real perturbations and will show that for this problem the complex assumption is only slightly conservative. This allows us to temporarily avoid resolving the tricky issue regarding the appropriate way to view the coefficient uncertainty.

Figure 4 shows the block diagram that includes all the features discussed above. It is clearly an example of Figure 1a, with e including e_{perf} and e_{act}, v including ϕ_{com}, gust, and sensor noise, and y including the measured outputs and ϕ_{com}. The dimensions of e, v, y, u, P, and Δ are 9, 6, 5, and 2, 17×17, and 9×3, respectively. State space models for the aircraft and the BrandX controller are included in the appendix.

Figure 4.

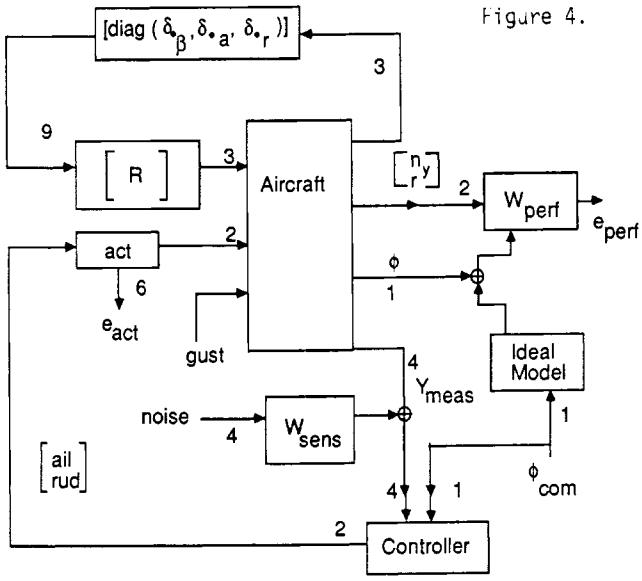

5. Brandx Robustness to Real Parameter Variations,
Nominal Performance, Robust Stability, Robust Performance

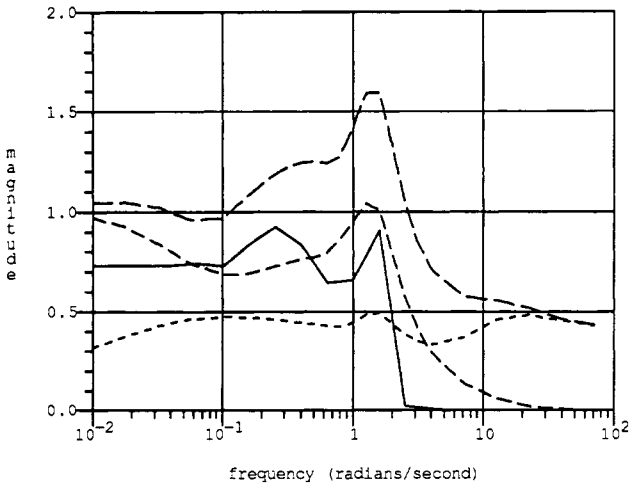

6. Musyn Robustness to Real Parameter Variations,
Nominal Performance, Robust Stability, Robust Performance

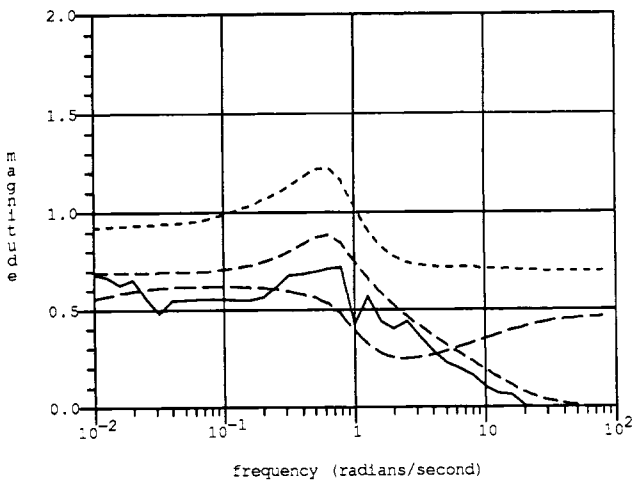

5. Comparisons of Designs

The μ plots of robustness and weighted performance for the BrandX design are shown in Figure 5. Referring to Figure 1b, the dashed plots are, from the top, $\mu(G)$ for robust performance, $\mu(G_{11})$ for robust stability, and $\bar{\sigma}(G_{22})$ for nominal performance. Note that the weights chosen for nominal performance make $\|G_{22}\|_\infty = .5$. If $\mu(G)$ were less than 1 then performance would only degrade by a factor of 2 for this level of uncertainty. Unfortunately, BrandX is unstable for the assumed uncertainty level because $\mu(G_{11}) > 1$ at $\omega \approx 1.5$. To give some idea of the sensitivity to the assumption that the δ's are complex, compare with the solid line which gives a lower bound for "real μ" for G_{11}. This lower bound was computed using two different programs (by M. Elgersma of SRC and M.K. Fan of U. of Maryland) which search for destabilizing real perturbations. These programs currently require that the Δ have only scalar blocks so each δ is assumed bounded in magnitude by 1. Note that since this lower bound is comparable to the complex $\mu(G_{11})$, we need not be particularly concerned about our assumptions on the δ's.

The corresponding plots for the Musyn design are shown in Figure 6. Robust stability and performance are improved at the expense of a slight degradation in nominal performance. Note that we now have robust stability for the assumed perturbations, but robust performance is not quite as desired. It is interesting to consider a controller designed using H_∞ optimization of G_{22}, ignoring the coefficient uncertainty. The nominal performance ($\bar{\sigma}(G_{22})$) of this controller, which we'll call Hinf, is plotted along with nominal performance of BrandX in Figure 7. Recall that Hinf is obtained by approximating the H_∞ optimal controller and so does not display the characteristic flat $\bar{\sigma}$ of theoretical H_∞ optimal designs, even though its norm is close.

The closeness of the BrandX and Hinf plots suggests two important points. First, the weight selection procedure was reasonably successful in capturing the BrandX performance. Had there been any "slack" in the weights (e.g. inadequate penalty on actuators or turn coordination or too small sensor noise), the Hinf design would have taken advantage of this to produce a much smaller norm. Secondly, BrandX is quite outstanding when viewed from this perspective. The $\mu(G_{11})$ plot of robust stability for Hinf in Figure 8 shows that it is destabilized by even tiny perturbations, but this is not too surprising since no robustness was asked for.

7. Brandx(X) and Hinf Nominal Performance

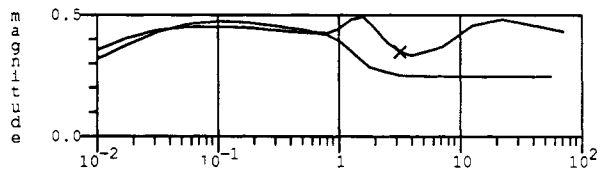

8. Hinf Design Robust Stability

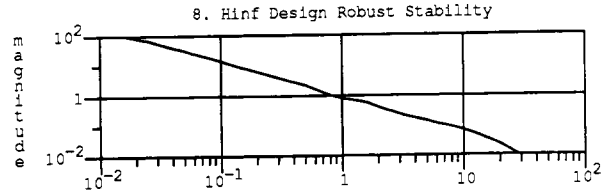

The μ plots may seem a bit mysterious to the uninitiated, and may actually obscure the important issue of robust performance. To get another view of these designs, consider Figure 9 which plots

$$\max_{\|\Delta\|_\infty \le \delta} \|F_\mu(G,\Delta)\|_\infty \quad \text{vs.} \quad \delta$$

where the max is taken over $\Delta \in \underline{\Delta}$. That is, the worst case performance over all $\|\Delta\|_\infty \le \delta$ is plotted vs. δ. Nominal performance is at $\delta = 0$ and there is a vertical asymptote at the δ_μ where the system goes unstable for some $\|\Delta\|_\infty = \delta_\mu$ (i.e. $\delta_\mu = 1/\mu(G_{11})$).

9. Performance/Uncertainty Trade-off
Brandx and Musyn

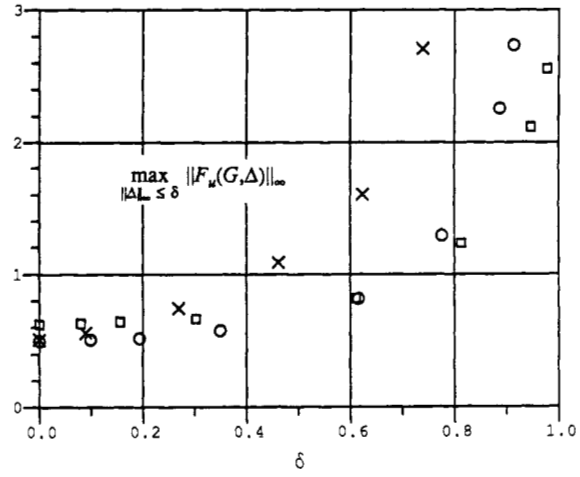

10. Musyn ○ Robustness to Real Parameter Variations,
Nominal Performance, Robust Stability, Robust Performance

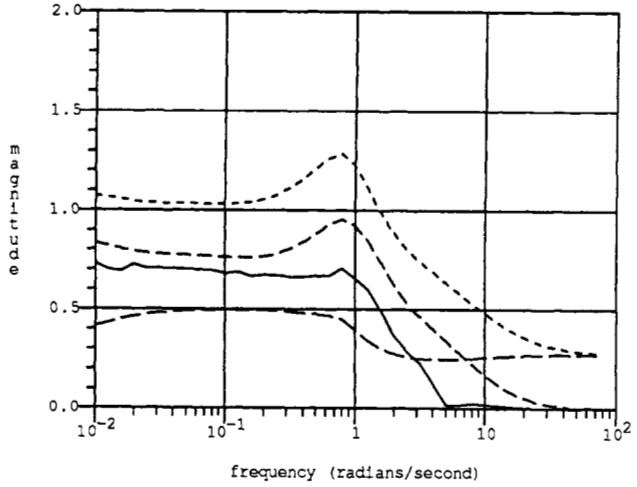

The symbols are × for BrandX, □ for Musyn, and ○ for an additional μ-synthesis controller designed with the perturbation weight reduced from 1 to .25. An exercise for aficianados: figure out how Figure 9 was made (hint: scale and compute μ). Note that □ has substantially better robust performance than BrandX but with slightly poorer nominal performance. ○ is a compromise that slightly beats BrandX nominally with slightly less robust performance than □. Hinf was not plotted since its robustness is so pathetic that $\delta_\mu \approx 0$. For comparison, the μ plots for ○ that correspond to Figures 5 and 6 are in Figure 10.

Some time domain comparisons of BrandX and Musyn are plotted in the figures below. Additional analysis of Musyn revealed that its most serious performance problem (the most significant contributor to $\|G_{22}\|$ or $\|e\|$), both absolute and relative to BrandX, is responses to the ϕ command. So to be fair, a step command of 28.6 deg (= .5 rad) in ϕ was chosen. Plots are shown of the response of ϕ, the turn coordination variables n_y and r_p, and the surface deflections. BrandX is denoted by an × and both nominal and perturbed conditions were considered. The perturbation is one for which BrandX is almost neutrally stable:

$$\begin{bmatrix} \delta_{\bullet\beta} & \delta_{\bullet a} & \delta_{\bullet r} \end{bmatrix} = \begin{bmatrix} 0 & 0 & 0 \\ 1.12 & 1.12 & .93 \\ 1.12 & -1.12 & 1.12 \end{bmatrix}$$

The time responses suggest the same conclusions as the μ analysis, that the nominal performance of the BrandX and Musyn controllers are quite similar, but the robustness characteristics are dramatically different. The contrast with Hinf would be even more dramatic. Of course, these time responses are only intended to be illustrative. No definitive conclusions of the sort provided by μ can be reached on the basis of a few time responses. On the other hand, since μ is fundamentally a frequency-domain analysis tool, its only direct implications for the time domain are in terms of L_2 or sinusoids.

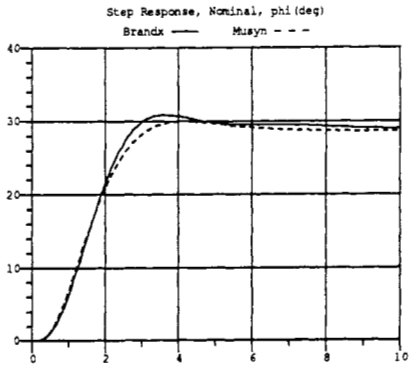

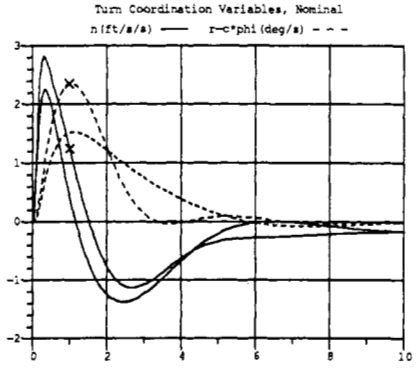

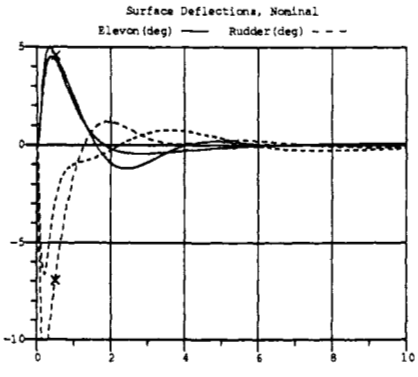

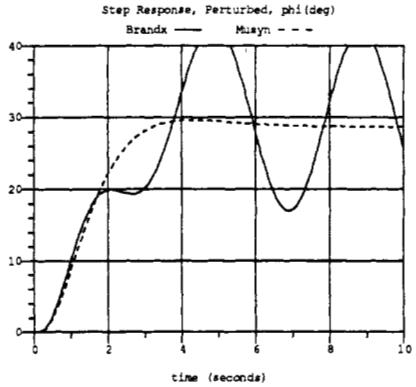

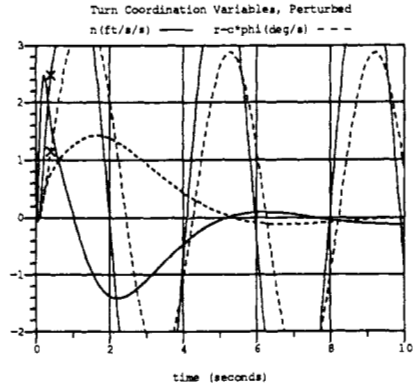

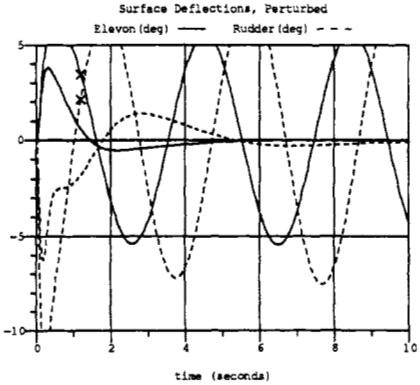

6. Conclusions

It is tempting to make wild claims, but it is important not to interpret the results in this paper too broadly. These results are extremely encouraging, and this study is certainly a success in demonstrating the applicability of μ to FCS design. Nevertheless, we must be cautious when drawing conclusions about the applicability of μ in general or about the relevance of this study to the Shuttle FCS.

Clearly, μ is a very powerful and promising tool, if only for analysis. Just the few plots shown in this paper yield important information about the performance and robustness of the controllers, and computation of μ has progressed to the point where it approaches that of singular values and eigenvalues in cost and reliability. While μ-synthesis is also very promising, it is highly experimental and will require additional study, application, and exposition before it can become a practical methodology.

While the issues treated in this paper are typical in the design of a FCS, much more careful and detailed study of the results would be required before making any serious conclusions about the Shuttle FCS. Even with immediate access to FCS experts and Shuttle data, in a brief study it is easy to overlook critical features of the problem. What is more important is that μ allows an engineer, in a systematic and reliable way, to explore tradeoffs and design for robustness wherever she believes it is significant. We view μ as the fundamental analytical tool at this time for treating performance and robustness in control systems.

The problem chosen was a challenging one because of its complexity and large, structured uncertainty. This is exactly the type of problem for which we would expect μ to show the greatest benefit. See [S1] for a similar study on a process control problem. In contrast, μ would have little impact on most SISO and many simpler MIMO problems. We expect that many more aerospace and process control problems will exhibit this level of complexity.

References

[C1] C.C. Chu and J.C. Doyle, "On inner-outer and spectral factorizations", *IEEE CDC*, Las Vegas, NV, 1984.

[C2] C.C. Chu, J.C. Doyle, and E.B. Lee, "The general distance problem in H_∞ optimal control", *Int. J. of Control*, 1986, Vol. 44, No.2.

[D1] J.C. Doyle, "Analysis of feedback systems with structured uncertainty", *IEE Proceedings*, Part D, No. 6, Nov., 1982.

[D2] J.C. Doyle, "Synthesis of robust controllers and filters", *IEEE CDC*, San Antonio, TX, 1983.

[D3] J.C. Doyle, "*Lectures Notes*", 1984 ONR/Honeywell Workshop on Advances in Multivariable Control, Oct. 8-10, 1984, Mpls., MN.

[D4] J.C. Doyle, "Structured uncertainty in control system design", *IEEE CDC*, Fort Lauderdale, FL, 1985.

[F1] B.A. Francis and J.C. Doyle, "Control theory with an H_∞ optimality criterion", *SIAM J. of Control*, 1986.

[M1] B.G. Morton and R.M. McAfoos, "A μ-test for real-parameter variations," *ACC Proceedings*,1985.

[M2] B.G. Morton and R.M. McAfoos, "New applications fo μ to real-parameter variation problems", *IEEE CDC*, Fort Lauderdale, FL, 1985.

[S1] S. Skogestad and M. Morari, "Control of ill-conditioned plants: high purity distillation columns", *AIChE Annual Meeting*, Miami Beach, FL, Nov., 1986.

Acknowledgements

The authors would like to thank the many people who contributed time and ideas to this paper, particularly B. Morton, R. McAfoos, D. Enns, G. Stein, and C.R. Stone, all of Honeywell SRC.

Appendix: Realizations of Aircraft and BrandX Controller

Aircraft Model

$$x_{state} = \begin{bmatrix} \beta \\ p \\ r \\ \phi \end{bmatrix} \quad y = \begin{bmatrix} c_\beta \\ c_a \\ c_r \\ y_{meas} \end{bmatrix} \quad u = \begin{bmatrix} c_y \\ c_n \\ c_l \\ u_a \\ u_r \\ gust \end{bmatrix}$$

Matrix : aircraft
outputs 7 inputs 6 states 4

	x1	x2	x3	x4	u1	u2	u3	u4	u5	u6
x1	-9.460e-02	1.409e-01	-9.900e-01	3.637e-02	1.275e-02	0.000e+00	0.000e+00	-1.240e-02	1.023e-02	-1.086e-04
x2	-3.595e+00	-4.284e-01	2.809e-01	0.000e+00	0.000e+00	-3.114e-02	-3.117e+00	6.571e+00	1.256e+00	-4.126e-03
x3	3.950e-01	-1.263e-02	-8.142e-02	0.000e+00	0.000e+00	-1.905e-01	-6.443e-02	3.783e-01	-2.560e-01	4.533e-04
x4	0.000e+00	1.000e+00	-1.405e-01	0.000e+00	0.000e+00	0.000e+00	0.000e+00	0.000e+00	0.000e+00	0.000e+00
y1	1.000e+00	0.000e+00	0.000e+00	0.000e+00	0.000e+00	0.000e+00	0.000e+00	0.000e+00	0.000e+00	1.148e-03
y2	0.000e+00	0.000e+00	0.000e+00	0.000e+00	0.000e+00	0.000e+00	0.000e+00	1.000e+00	0.000e+00	0.000e+00
y3	0.000e+00	0.000e+00	0.000e+00	0.000e+00	0.000e+00	0.000e+00	0.000e+00	0.000e+00	1.000e+00	0.000e+00
y4	0.000e+00	1.000e+00	0.000e+00	0.000e+00	0.000e+00	0.000e+00	0.000e+00	0.000e+00	0.000e+00	0.000e+00
y5	0.000e+00	0.000e+00	1.000e+00	0.000e+00	0.000e+00	0.000e+00	0.000e+00	0.000e+00	0.000e+00	0.000e+00
y6	-6.804e+01	-1.744e+00	-4.058e+00	-3.720e-05	1.111e+01	-1.111e+01	-1.111e+01	2.667e+01	-2.952e+00	-7.810e-02
y7	0.000e+00	0.000e+00	0.000e+00	1.000e+00	0.000e+00	0.000e+00	0.000e+00	0.000e+00	0.000e+00	0.000e+00

Brandx Controller

$$y = \begin{bmatrix} u_a \\ u_r \end{bmatrix} \quad u = \begin{bmatrix} \phi_{com} \\ Y_{meas} \end{bmatrix}$$

Matrix : control
outputs 2 inputs 5 states 3

	x1	x2	x3	u1	u2	u3	u4	u5
x1	-1.000e-05	0.000e+00	0.000e+00	1.662e-01	-1.990e-01	1.033e-02	-9.109e-04	-1.656e-01
x2	0.000e+00	-1.000e-05	0.000e+00	-4.418e-02	-3.232e-02	5.960e-01	1.448e-03	2.258e-02
x3	0.000e+00	0.000e+00	-1.250e+00	-4.899e-09	7.652e-09	-1.286e-08	-9.824e-02	5.329e-09
y1	2.936e-01	1.847e-01	5.026e-13	1.615e-01	-2.560e-01	4.496e-01	1.862e-14	-1.767e-01
y2	-9.253e-02	5.697e-01	-1.128e-01	-4.037e-01	-6.507e-12	3.371e+00	-5.389e-04	2.806e-01